

Active Mercury(II) Ion Removal: Stoichiometrically Controlled Thiol-Functionalized Mesoporous Silica by a Mass Production Spray Dry System

Yusuke Yamauchi,*[1,2] Norihiro Suzuki,[1] Keisuke Sato,[1] Naoki Fukata,[1] Miwa Murakami,[3] and Tadashi Shimizu[3]

[1]World Premier International (WPI) Research Center for Materials Nanoarchitectonics (MANA), National Institute for Materials Science (NIMS), 1-1 Namiki, Tsukuba 305-0044

[2]PREST, JST, 5 Sanban-cho, Chiyoda-ku, Tokyo 102-0075

[3]High-field NMR Group, Advanced Nano Characterization Center, 3-13 Sakura, Tsukuba 305-0003

Received March 5, 2009; E-mail: Yamauchi.Yusuke@nims.go.jp

Stoichiometrically controlled thiol-functionalized mesoporous silica particles are synthesized by a spray dry technique in one step. The EDS (energy dispersive X-ray spectrometer) mapping shows that thiol groups are well dispersed throughout the particles without phase separation at micrometer scale. From TEM (transmission electron microscope) observation, SAXS (small-angle X-ray scattering) measurements, and N_2 adsorption–desorption isotherms, it is proven that the thiol groups can be successfully embedded in the frameworks up to 30% without any collapse of ordered mesoporous structures. The amount of the embedded thiol groups in the final products can be stoichiometrically controlled by changing the compositions of the initial precursor solutions, as is confirmed by ^{29}Si NMR measurements. The total adsorption capacity of mercury(II) ions was increased in proportion to the amount of the thiol groups embedded in the frameworks.

In the modern world, environmental pollution caused by human activity is a serious problem. Heavy metal ions originating from factories, mines, and industrial wastes have accumulated in soil and water, resulting in serious pollution. Because of the toxicological effects on living things, heavy metal ion contamination is a significant threat to us. For example, mercury(II) ion may form organomercury compounds, which are often extremely toxic and cause brain and liver damage. Unlike organic pollutants, heavy metals do not decompose and thus an efficient adsorbent for heavy metal ion removal is required immediately.

Mesoporous silica is one of the best candidates for adsorbent materials due to unique features such as very high surface area and large pore volume. To further enhance functional properties, mesoporous organosilica, which contains organic fragments in the silica framework, has been synthesized.[1–9] As for the heavy metal ion removal, intercalation of organic fragments interacting with heavy metal ion is important. Because thiol and thiourea groups are known to exhibit interaction with mercury(II) ion, the synthesis of thiol- or thiourea-functionalized organosilica has been conducted by many groups.[10–16] In order to finely control the heavy metal ion adsorption ability, stoichiometrically controlled synthesis of functionalized mesoporous organosilicas should be important. However, in conventional co-condensation processes in micellar solution, the organic content in products is usually not consistent with that in the precursor solutions.[17,18] For stoichiometrically controlled synthesis, special conditions such as very dilute conditions[13,15] and high surfactant concentration[16] are required.

Recently, several spherical mesoporous particles (e.g., silica,[19–23] organosilica,[3,7,14] maghemite–organosilica,[24] carbon,[25] and metal oxide[26]) have been prepared by aerosol-assisted processes. The important advantage of spray drying is the product compositions can be stoichiometrically controlled by changing the compositions of the initial precursor solutions. In this process, the liquid feed (i.e., precursor solution) is sprayed through a nozzle into a hot steam gas in which the supplied liquid is vaporized and the droplets are dried immediately. However, the previous system is not suitable for continuous production, because the dried samples are collected by membrane filters. Very recently, we newly developed a laboratory-made apparatus for rapid and large-scale production.[27] In our system, the dried samples can be collected with a cyclone separator due to strong centrifugal force. Therefore, our spray drying process can be used for long hours without any complex post-processing, making it suitable for industrial applications.

In this paper, our system is extended to the preparation of thiol-functionalized mesoporous organosilica particles for mercury(II) ion removal. In particular, we focus on stoichiometric controls of thiol contents in the frameworks to finely control the amount of adsorbed mercury(II). No collapse of the ordered mesostructures were observed up to 30% thiol content embedded in the frameworks, though disorder occurred by embedding 20% thiol content in a previous spray dry production.[14] Also, the activity of mercury(II) adsorption (per thiol group) did not decrease at all, even though the thiol content increased. To the best of our knowledge, the systematic

Published on the web August 7, 2009; doi:10.1246/bcsj.82.1039

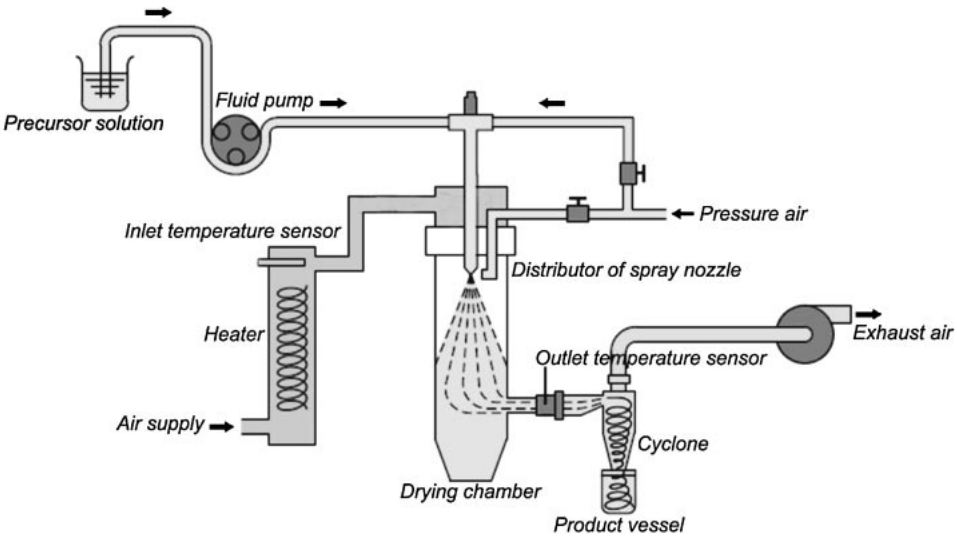

Figure 1. The system diagram of the laboratory-made spray dryer apparatus.

spray dry system focusing on stoichiometric control has not been reported so far, though several spray-dried mesoporous materials with different compositions have been designed by adjusting the composition of the precursor solutions.[3,7,14,19–26]

Experimental

Materials. Extra pure TEOS (tetraethyl orthosilicate) as a silica source, hydrochloric acid (pH 2), and 36% hydrochloric acid solution were purchased from Nacalai Tesque, Inc. Ethanol (purity = 99.5%, Koso Chemical Co., Ltd.) was used as a solvent. A triblock copolymer (Pluronic F127, PPO_{106}–PPO_{70}–PEO_{106}) and $Hg(NO_3)_2$ aqueous solution (0.01 mol L^{-1}) were obtained from Aldrich Co. 3-MPTMS ((3-mercaptopropyl)trimethoxysilane) purchased from Kanto Chemical Co., Inc. was used as a thiol source.

Laboratory-Made Spray Dryer Apparatus. Based on the Spray Dryer GB22 (Yamato Scientific Co.), we handmade an apparatus for this study (Figure 1). A two-flow spray nozzle (inside and outside diameters are 406 and 1270 μm, respectively) is used for droplet generation. The nozzle tip pressure is tunable from 0.05 to 0.30 MPa. Inlet temperature of the drying chamber can be controlled from 50 to 280 °C. The digital temperature display is accurate to ±1 °C. Spray-dried samples are collected in a cyclone collector by utilizing the centrifugal force generated in the cyclone. Temperature resistant, super hard glass is used for the drying chamber, the cyclone, and the cyclone collector.

Preparation of Precursor Solutions. The precursor solutions were prepared by mixing TEOS, 3-MPTMS, and 2.5 g of ethanol in a beaker and then adding 3.1 mL of HCl (pH 2) solution dropwise. Three types of precursor solution were prepared by varying the amount of 3-MPTMS. For comparison, the pure mesoporous silica particles were also prepared by using TEOS only. The amount of both TEOS and 3-MPTMS in each sample are summarized in Table 1. The mixture was vigorously stirred for about 30 min until the mixture became clear. 2.5 g of ethanol and 2.0 g of Pluronic F127 (surfactant) were mixed and shaken vigorously for about 30 min in another beaker. After that, two solutions were mixed. After stirring for 30 min, the clear precursor solutions were obtained.

Spray-Dry Synthesis. The precursor solutions were spray dried under the following conditions: the aspirator rate: 0.45 $m^3\,h^{-1}$, the inlet temperature: 250 °C, and the nozzle pressure: 0.20 MPa. The droplets of the solutions were carried by an air flow and evaporated in the drying chamber, followed by collecting particles with the cyclone collector. To remove the surfactant, these particles were washed twice in a mixture of 3.8 g of 36% HCl aqueous solution and 150 mL of ethanol.

Table 1. The Compositions of the Precursor Solutions

	TEOS /g	TEOS /mol	3-MPTMS /g	3-MPTMS /mol	Percentage of 3-MPTMS to TEOS/%
Sample A	6.5	0.031	0	0	0
Sample B	6.5	0.031	0.6	0.0031	10
Sample C	6.5	0.031	1.2	0.0062	20
Sample D	6.5	0.031	1.8	0.0094	30

Characterization Techniques. The spray-dried samples were observed on a Hitachi S-4800 field emission scanning electron microscope. The TEM images were obtained using a JEOL-3000F. The accelerating voltage of the electron beam was 200 kV. Powder samples for the TEM observation were dispersed in ethanol by ultrasound and mounted on a microgrid. The small-angle X-ray scattering (SAXS) spectra were measured by NANO-Viewer (Rigaku). Nitrogen adsorption–desorption isotherms were measured by using a Quantachrome Autosorb-1. All samples were outgassed at 100 °C for 24 h before the measurement. The specific surface area and the pore size were calculated using Brunauer–Emmett–Teller (BET) and Barrett–Joyner–Halenda (BJH) methods, respectively. Solid-state ^{1}H-decoupled ^{29}Si magic angle spinning (MAS) nuclear magnetic resonance (NMR) measurements were performed on a JEOL-ECA 500 (11.7 T) spectrometer at a spinning rate of 8 kHz and a resonance frequency of 99.37 MHz with a 45° pulse length of 1.8 μs and a recycle time of 120 s. Micro-Raman scattering measurements were performed to investigate S states at room temperature with a 100× objective and a 532-nm excitation light. The excitation power was set to be about 10 mW. The spectral resolution of all data are about 0.3 cm^{-1}. The mercury ion adsorption capacity was examined by reduction aeration atomic absorption spectroscopy. 15 mg of the spray-dried samples was added into 10 mL of $Hg(NO_3)_2$ aqueous solution (0.01 mol L^{-1}) and left at rest for 1 h. 50 μL of the clear supernatant

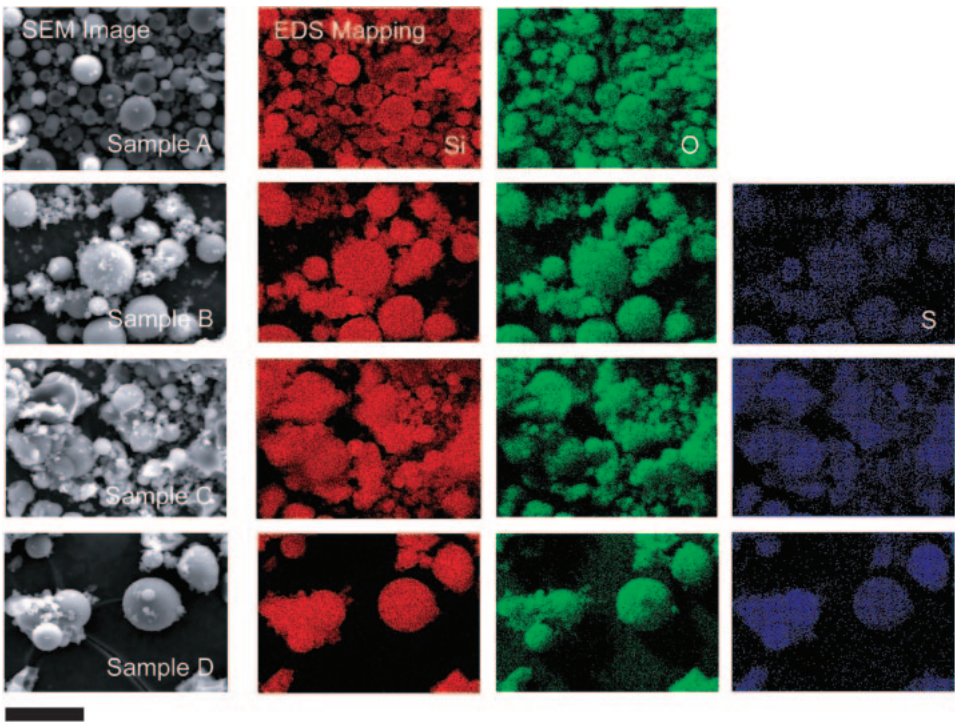

Figure 2. SEM images and EDS mappings (Si, O, and S) of the samples after removal of surfactants. Scale bar is 20 μm.

liquid was taken and diluted with pure water. The mercury concentration of the diluted solution was measured by a fully-automatic heat-vaporization mercury measuring instrument (MA-2000, Nippon Instruments Corporation), then the amount of mercury(II) adsorbed to the thiol-functionalized silica sample was calculated.

Results and Discussion

The SEM images of the spray-dried samples prepared by various precursor solutions are shown in Figure 2. These images showed that the samples have spherical morphology. These facts indicate that the spherical droplets generated from the nozzle uniformly shrunk into the center point in the drying chamber. The spherical morphology was retained after removing the surfactant. EDS mapping showed that thiol groups were well dispersed throughout the particles without phase separation at micrometer scale.

In the Figure 3, the SAXS patterns of the samples after removal of the surfactants are displayed. A prominent peak corresponding to the mesoscopic periodicity was observed in each sample and the estimated pore–pore distance was 12.4 (Sample A), 11.8 (Sample B), 11.5 (Sample C), and 11.7 nm (Sample D). The basal spacings were not changed, that is, the amount of the thiol groups embedded in the framework did not affect the mesoscopic periodicity.

The mesoscopic ordering was also observed by TEM. Figure 4 shows the TEM images of Sample D with high thiol contents. It was observed that the cage-like spherical mesopores were formed within the spray-dried particles and they were closely packed with each other. By tilting the TEM sample grid, similar cage-like spherical mesopores were observed (Figure S1). This fact also nicely supports the formation of spherical mesopores. The pore-to-pore distance

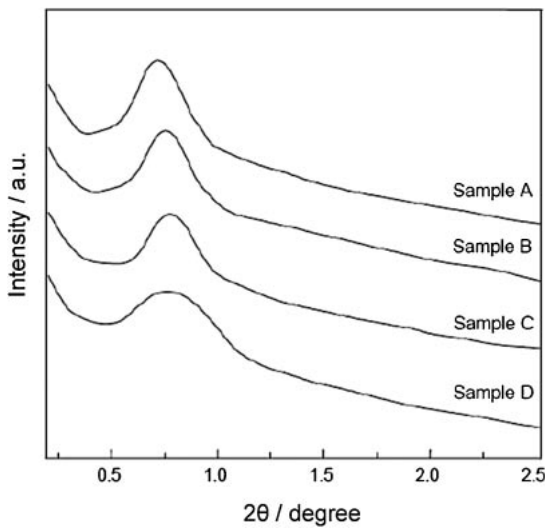

Figure 3. The SAXS spectra for the samples after removal of surfactants.

is estimated to be about 12 nm, which is in good agreement with the SAXS data. From the EDS mapping analysis and corresponding TEM (Figure 4b), it was shown that the thiol groups were uniformly dispersed. No phase separations at nanometer scale were observed at all. In addition, the presence of the thiol groups were evidenced by the detection of S–H stretching bands in the Raman spectrum (2570 nm).[10,15] However, an S–S streching band (510 nm) was not detected, indicating the absence of thiol group oxidation in these samples (Figure S2).

The N_2 adsorption–desorption isotherms and the pore-size distributions are summarized in Figure S3. The isotherms

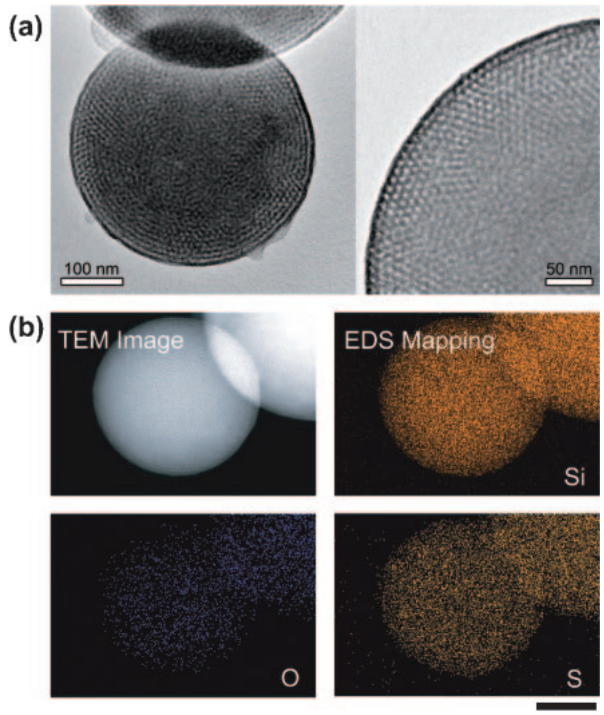

Figure 4. (a) TEM images and (b) EDS mappings (Si, O, and S) of Sample D with high thiol contents. Scale bar is 1 μm.

showed type IV with a hysteresis loop. Large N_2 uptake was observed at low relative pressures. This indicates the presence of micropores (less than 2 nm), originating from the hydrophilic tails of the triblock polymer. The average pore sizes calculated by a BJH method decreased with the increase in the amount of thiol groups, which is caused by the increased coverage of thiol groups on the surface of the mesopores.[10] Samples A, B, and C exhibited high BET surface areas, while the BET surface area of Sample D decreased due to the increased coverage of thiol groups on the pore surface. This tendency has been reported by Nakamura et al.[15]

The ^{29}Si cross-polarization magic-angle spinning (MAS) NMR spectra are shown in Figure 5. For Sample A, three peaks appeared at −108.1 (Q^4), −100.8 (Q^3), and −91.5 ppm (Q^2). These peaks are attributed to silicon atoms without hydroxy group [$(SiO)_4$–Si], with one hydroxy group [$(SiO)_3$–Si–OH], and with two hydroxy groups [$(SiO)_2$–Si–$(OH)_2$], respectively.

In other samples, the T^3 and T^2 peaks were observed. The T^3 and T^2 peaks are attributed to [$(SiO)_3$–SiR] and [$(SiO)_2$–SiR–(OH)] (where R represents the thiol group derived from 3-MPTMS). The observed T^3 peaks were at −64.4 (Sample B) and −65.4 ppm (Samples C and D). The T^2 peak for Samples B, C, and D were located at −58.0, −56.6, and −57.1 ppm, respectively. In Samples C and D, the area intensity of thiol group derived peaks (i.e., T^2 and T^3) were doubled and tripled in comparison with that of Sample B, though the silica derived peak areas (i.e., Q^2, Q^3, and Q^4) were almost constant among Sample B, C, and D. This means the stoichiometry was maintained after the spray-dry synthesis (See the initial compositions, Table 1).

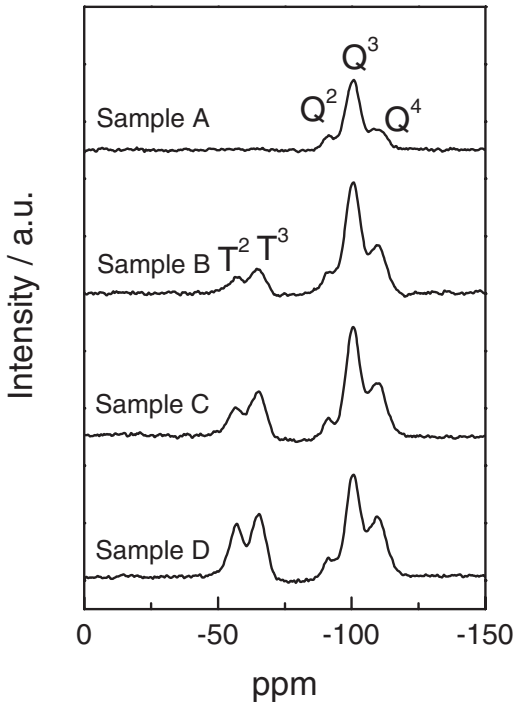

Figure 5. The ^{29}Si cross-polarization MAS NMR spectra.

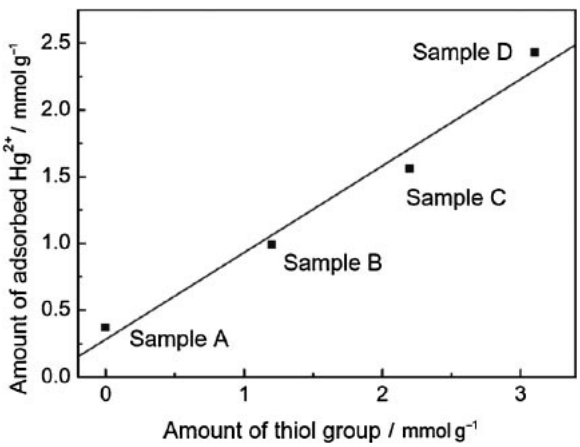

Figure 6. The relationship between the amount of the adsorbed mercury(II) ion and the amount of thiol groups embedded in the frameworks. Each amount (mol) was normalized to the total sample amount (g).

The relationship between the adsorbed mercury(II) ion and the amount of thiol groups is shown in Figure 6. In the absence of thiol groups, slight adsorption of mercury(II) onto mesoporous pure silica was observed due to the physisorption into the mesoporous matrix with high surface area. The total adsorption capacities increased in proportion to the amount of thiol groups in the samples. Furthermore, the amounts of adsorbed mercury(II) were normalized to the number of thiol units. The adsorption capacities per thiol unit were estimated to be 0.82 (Sample B), 0.69 (Sample C), and 0.77 (sample D), respectively. Considering the physisorption, the values were 0.51 (Sample B), 0.53 (Sample C), and 0.66 (Sample D), respectively. The adsorption capacities per thiol unit were almost the same or slightly higher than reported in previous

papers using HMS mesoporous organosilica with much lower thiol contents.[10] This enhancement was probably because of the exposure of a thiol group caused by the existence of micropores. Here we successfully demonstrated that high thiol content organosilica can be synthesized without loss of mercury(II) adsorption by using a spray-dry technique. Although the obtained spray-dried samples were mixed with $Hg(NO_3)_2$ aqueous solution for 1 h in this experiment, the adsorption rates for all the samples were fast. Actually, it took only 20 min to completely adsorb the saturated amount of mercury(II).

In addition, the spray-dried samples in this study showed good hydrothermal stability. It has been generally known that mesoporous silica materials prepared by block copolymers such as P123 and F127 have significantly greater hydrothermal stability in comparison with conventional MCM-41 materials using cationic surfactants, due to thick frameworks. The thiol-functionalized mesoporous organosilica prepared by using CTAB showed a well-resolved SAXS pattern, but after heating in boiling water for 12 h, the material becomes amorphous and loses all reflections. In contrast, all of the samples prepared with F127 block copolymers are very stable after heating in boiling water longer than 12 h, and the surface area and pore size were unchanged and detachment of thiol groups was not observed by the EDS mapping. Such excellent stability is very important from the viewpoint of the removal of heavy ions in water.

Conclusion

Using a spray-drying technique, we produced thiol-functionalized mesoporous organosilica particles in one step. The stoichiometory was well retained during the fabrication. Up to 30%, the embedded groups did not effect the ordered structure. The ability to remove mercury(II) was proportional to the amount of thiol groups in the organosilica particles. This paper demonstrated the synthetic platform for the preparation of stoichiometrically controlled functionalized mesoporous organosilica. This useful and inexpensive system allows production of many types of organosilica with other functional groups, which could be important nanoporous materials as adsorbents of other heavy metal ions in the future.

Supporting Information

Figure S1: The TEM image of Sample D, Figure S2: Raman spectra for Sample D, and Figure S3: The N_2 adsorption–desorption isotherms and the pore-size distributions of each sample. This material is available free of charge on the web at http://www.csj.jp/journals/bcsj/.

References

1 S. Inagaki, S. Guan, Y. Fukushima, T. Ohsuna, O. Terasaki, *J. Am. Chem. Soc.* **1999**, *121*, 9611.

2 S. Guan, S. Inagaki, T. Ohsuna, O. Terasaki, *J. Am. Chem. Soc.* **2000**, *122*, 5660.

3 Y. Lu, H. Fan, N. Doke, D. A. Loy, R. A. Assink, D. A. LaVan, C. J. Brinker, *J. Am. Chem. Soc.* **2000**, *122*, 5258.

4 Ö. Dag, C. Yoshina-Ishii, T. Asefa, M. J. MacLachlan, H. Grondey, N. Coombs, G. A. Ozin, *Adv. Funct. Mater.* **2001**, *11*, 213.

5 Y. Liang, M. Hanzlik, R. Anwander, *Chem. Commun.* **2005**, 525.

6 Y. Goto, S. Inagaki, *Microporous Mesoporous Mater.* **2006**, *89*, 103.

7 X. Ji, Q. Hu, J. E. Hampsey, X. Qiu, L. Gao, J. He, Y. Lu, *Chem. Mater.* **2006**, *18*, 2265.

8 Y. Wan, D. Zhang, Y. Zhai, C. Feng, J. Chen, H. Li, *Chem. Asian J.* **2007**, *2*, 875.

9 Y. Luo, P. Yang, J. Lin, *Microporous Mesoporous Mater.* **2008**, *111*, 194.

10 J. Brown, L. Mercier, T. J. Pinnavaia, *Chem. Commun.* **1999**, 69.

11 A. M. Liu, K. Hidajat, S. Kawi, D. Y. Zhao, *Chem. Commun.* **2000**, 1145.

12 V. Antochshuk, M. Jaroniec, *Chem. Commun.* **2002**, 258.

13 H.-Y. Wu, C.-H. Liao, Y.-C. Pan, C.-L. Yeh, H.-M. Kao, *Microporous Mesoporous Mater.* **2009**, *119*, 109.

14 I. V. Melnyk, Y. L. Zub, E. Véron, D. Massiot, T. Cacciaguerra, B. Alonso, *J. Mater. Chem.* **2008**, *18*, 1368.

15 T. Nakamura, Y. Yamada, K. Yano, *J. Mater. Chem.* **2007**, *17*, 3726.

16 D. Liu, J.-H. Lei, L.-P. Guo, X.-D. Du, K. Zeng, *Microporous Mesoporous Mater.* **2009**, *117*, 67.

17 C. E. Fowler, S. L. Burkett, S. Mann, *Chem. Commun.* **1997**, 1769.

18 R. Richer, L. Mercier, *Chem. Commun.* **1998**, 1775.

19 Y. Lu, H. Fan, A. Stump, T. L. Ward, T. Rieker, C. J. Brinker, *Nature* **1999**, *398*, 223.

20 N. Andersson, P. C. A. Alberius, J. S. Pedersen, L. Bergström, *Microporous Mesoporous Mater.* **2004**, *72*, 175.

21 S. Areva, C. Boissière, D. Grosso, T. Asakawa, C. Sanchez, M. Lindén, *Chem. Commun.* **2004**, 1630.

22 S. H. Kim, B. Y. H. Liu, M. R. Zachariah, *Langmuir* **2004**, *20*, 2523.

23 M. H. Sörensen, R. W. Corkery, J. S. Pedersen, J. Rosenholm, P. C. Alberius, *Microporous Mesoporous Mater.* **2008**, *113*, 1.

24 B. Julián-López, C. Boissière, C. Chanéac, D. Grosso, S. Vasseur, S. Miraux, E. Duguet, C. Sanchez, *J. Mater. Chem.* **2007**, *17*, 1563.

25 Y. Yan, F. Zhang, Y. Meng, B. Tu, D. Zhao, *Chem. Commun.* **2007**, 2867.

26 C.-K. Tsung, J. Fan, N. Zheng, Q. Shi, A. J. Forman, J. Wang, G. D. Stucky, *Angew. Chem., Int. Ed.* **2008**, *47*, 8682.

27 Y. Yamauchi, T. Kimura, *Chem. Lett.* **2008**, *37*, 892.